School of Physics and Astronomy

WATCHMAN: Neutrinos for Nuclear Non-Proliferation

MPhys Project

Larisa Dorman-Gajic
March 2021

Abstract

A neutrino detector investigating the outputs from near by, 26km away, nuclear reaction is being built to investigate the possible use of neutrino detection for non-proliferation goals. This detector is called WATCHMAN and is being built in Boulby, UK. WATCHMAN will be a test to see if characteristics of the detector can be used for larger scales. This will be done with two different detector mediums, possibly at different stages of the WATCHMAN experiment. This paper investigates a new method of energy reconstruction for the outputs of the detector, using a machine learning framework to predict the energy of an event from given parameters. This paper investigates the possible use of this framework for future use in WATCHMAN by analysing varying event energies and positions. The results from this paper give a mean gain in energy resolution using this method of 2.2±1.9% for a new 3% water based liquid scintillator medium, and energy resolution gains of 6.6±5.3% for the more well studied Gadolinium-doped water medium.

Declaration

I declare that this project is my own work.

Signature: Date: April 16, 2021

Supervisor: Dr M. D. Needham 24 Weeks

Personal Statement

Before I began the project I did a basic C++ coding course on Udemy. This was due to the use of this language throughout the WATCHMAN project. Previously, I had only coded in Python so I needed to learn how to write and utilise C++. I also cloned all the appropriate modules from the AIT-WATCHMAN git-hub.

In the first 6 weeks of the project I practiced using the modules from AIT-WATCHMAN as well as reading papers provided by my supervisor. In this time I was also added to the WATCHMAN Wiki where updates of the project were put. Here I went through the slides of the 'SAS Workshop' which talked me through the modules used in the project. I tried out initial simulations and had weekly meetings with my supervisor to discuss the outcomes of them.

There were issues while trying to reconfigure the output files from the modules used. This was due to changes being made to these modules. After correspondence with members of the wider team I managed to get the code to reconfigure the outputs into the right format working.

After this, I was doing continuous simulations, taking data on the workings of the simulation code and detector.
In the week before and after Christmas break I discussed with my supervisor, other members of the Edinburgh WATCHMAN team, and a phd student in Sheffield about where my project could expand further. The WATCHMAN project has many contributors so we had to make sure I wasn't doing something that was already being attempted in another area of research for the project. In these discussion I decided that going down a machine learning route would be an interesting course of action, and one not yet used for energy reconstruction for WATCHMAN.

I have never worked with machine learning before so I spent a few weeks reading up on it and talking with a member of the Edinburgh WATCHMAN team who had experience with use of machine learning in particle physics experiments. I then wrote scripts for implementing machine learning into my data analysis.

I decided at this time to use a different detector medium that was looking increasingly likely to be used in the future detector. For the rest of the project I tweaked simulations, running them for many different parameters. I then analysed my findings discussion plausibility with my supervisor.

At the final stage I put together all of my data and finished writing my report.

Acknowledgements

I want to thank my supervisor Matthew Needham as well as Gary Smith, and Evangelia Drakopoulou from the University of Edinburgh for vital advice throughout this project.

I would also like to thank the entire WATCHMAN team in giving me insights into an exciting project that has taught me a lot.

Finally, I would like to thank Steve Wilson from the University of Sheffield who has given me guidance on the data analysis of this project.

I worked on WATCHMAN previously for my Senior Honors Project last year. There, I focused on PMT performance for use in the detector. In this project I have been on the simulation side of the project.

Contents

1 Introduction

This project involves the development of a new method for energy reconstruction of neutrino events within a neutrino detector, called WATCHMAN[1], that is being built in the UK. The method implements machine learning from a Scikit-Learn package called Gradient Boosting Regressor[2] to increase the energy resolution of detected events as well as speed up the event analysis process. As well as this two detector mediums, which have been proposed for WATCHMAN[1], are explored. These mediums are Gadolinium-doped water, which uses the Cherenkov effect, and a water based liquid scintillator, which uses both Cherenkov and scintillation light to detect neutrinos.

Neutrino physics is currently one of the largest research areas within particle physics[3]. In addition to this, it also has a strong bearing on nuclear, astrophysics, and cosmology due to the frequent production of neutrinos in many diverse events. Neutrinos are released in large numbers in stars and supernovae; from naturally occurring nuclear reactions on Earth; as well as, from man made sources such as nuclear reactors and military uses[4]. Neutrinos are very light, neutral particles, this means that they are extremely difficult to detect and only interact via gravity and weak interactions (through exchanges of Z and W bosons)[5]. This difficulty is helped by building neutrino detectors underground[5], keeping out as much background signal as possible. Neutrinos being released from all nuclear sources means that their detection would give us a better understanding[6] of where man made nuclear sources are occurring and the state in which they are in. Also, due to neutrinos minimal interaction it is an impossibility for an organisation or government to stop neutrinos from escaping from a reactor[6]. This means that there is an opportunity to gain insight of these man-made nuclear reactions from far afield.

The monitoring of antineutrinos has been proposed for non-proliferation goals, non-proliferation being the prevention of the spread of nuclear weapons[6] [7]. However, neutrino detection is not yet advanced enough to operate at large distances[7]. Hence, new physics is being developed[8] to see the ability of accurate detection of neutrinos near nuclear reactors with known reaction timings. The thermal power released in the fission process within the reactor is directly related to the flux of the anti-neutrino emitted[6]. Due to the weak interactions of neutrinos they escape the reactor containment causes no significant change in numbers and energies[6]. In measuring the flux of anti-neutrinos nearby, information of the reactor's status and power can be documented. This is the aim for a proposed WATer CHerenkov Monitor of ANtineutrinos (WATCHMAN)[8] detector that is to be located in Boulby, 26 km from a two-reactor complex in Hartlepool in north England[1]. WATCHMAN will monitor the on and off switching of a nearby nuclear power station in Hartlepool, hopefully, being able to determine its activities without prior knowledge of them. This would demonstrate the effectiveness of this method and will show that this detector design is scaleable[8] for monitoring nuclear reactions. WATCHMAN will be a cylindrical tank, with a height and diameter of 20 metres, lined with around 3000 10-inch photomultiplier tubes[9]. Photomultiplier tubes being large bulb shaped photon detectors which use the photoelectric effect to measure photon energy.

For WATCHMAN to carry out its goals it need precise event reconstructions. The neutrinos being measured will be used to track the workings of nuclear reactions and hence the detector must be very sensitive to any changes in energies. Due to this, this project's goal is to increase the energy resolution of the WATCHMAN detector. This is done via the simulation of the detector and events within it using a package called RAT-PAC[10] and then using the output data to reconstruct events within a machine learning framework. Tests of the energy resolution of the detector are done for various energies and locations within the tank. Initial tests are done first to see the trends of the detector using the current method of energy reconstruction. Then, a new method was developed and used to analyse the simulated events.

2 Neutrino Detectors

Neutrinos get released from all nuclear reactions[11], such as those within the sun and nuclear power plants. Due to their size and lack of charge neutrinos are extremely weakly interacting[12] making them hard to detect. Detectors are built deep underground to try to isolate the detector from a variety of background sources which may mimic the signature of a neutrino[13].

Neutrinos, only interacting via gravity and the weak force[12], limit the techniques in which we can detect them. Due to their extremely small rest mass, detection through gravitational means is not possible (at least not with our current technology), this leaves the weak interaction[12] as the only feasible source of detection. Neutrinos interact via the weak force in two ways; neutral-current interactions, occurring through the exchange of a Z^0 boson, where the neutrino transfers momentum to a lightweight charged particle[11]; and charged-current interactions. Charged-current interactions require more energetic neutrinos to occur. They happen through the exchange of a $W^{\pm}$ boson when a neutrino interacts with a hadron to a different hadron and an equivalent charged lepton[11]. An example of this is the inverse beta decay[12]:

$$\bar{\nu}_e + p \rightarrow e^+ + n \tag{1}$$

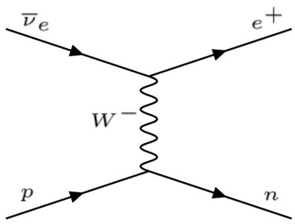

Figure 1: Feynman diagram of the Inverse Beta Decay[14]

This reaction occurs when an anti-neutrino interacts with a proton via the weak force (seen in 1 as the virtual W^- boson) resulting in a fast moving positron and a thermal neutron[12]. It is the outputs of this reaction which the detector uses to indicate the presence of the anti-neutrino[15].
Which method of neutrino detection an experiment uses is dependent on the requirements

of the study. For WATCHMAN anti-neutrinos will be detected through the products of the inverse beta decay[8].

The neutrino interaction outputs produce gamma rays[12], and neutrino detectors such as WATCHMAN use PMTs to detect these gamma rays within the a detector medium. PMTs consist of a glass vacuum tube using photocathodes and electron multipliers to produce a signal when exposed to a gamma ray. When a photon enters the glass dome it excites an electron in the photocathode, which accelerates and is repeatedly multiplied over multiple diodes, creating a measurable current. This process uses the well known photoelectric effect, which converts energy from photons to photoelectrons through a quantum mechanically process. This allows for the energy from the photon hitting the PMT to be measured accurately. The PMTs used in WATCHMAN are the 10 inch (220mm) Hamamatsu R7081[9] PMTs with low radioactivity glass.

3 WATCHMAN

WATCHMAN is a far field test for the Advanced Instrumental Testbed[1] (AIT). AIT is group of technologies used to monitor nuclear reactors. AIT-WATCHMAN is a large collaboration of universities and institutions from the UK and USA with Lawrence Livermore National Laboratory (LLNL) having overall responsibility[1] for its delivery. WATCHMAN's goals are to; confirm the existence of a reactor power station 26km away in Hartlepool; then to, determine its operational status both with and without prior knowledge of the reactor cycle. As well as this it wishes to demonstrate the scaleablility[1] of the reactor and reactor medium, and provide future analysis in anti-neutrino detection[8].

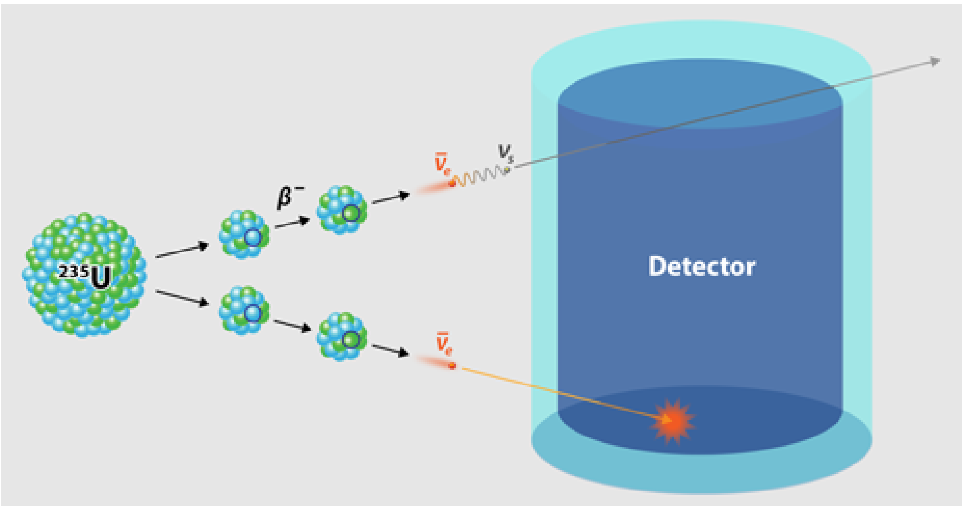

Figure 2: Visual of how the neutrinos get produced within the reactor and how they make their way to the detector.[16]

The Hartlepool Power Station is a two reactor complex in north England[1] which produce a combined electrical output of 1190MW. WATCHMAN will measure the power stations outputs for various on and off modes of these two reactors which contain 110 tonnes of Uranium[1] each with a ^{235}U enrichment varying between 2-4%. The neutrinos that will get detected in WATCHMAN are electron anti-neutrinos, $\bar{\nu}_e$. They originate in reactor cores during the beta decay of fission by products[17], with, on average, 6 electron anti-neutrinos getting released per fission[11][17]. The $\bar{\nu}_e$ energy is usually below 10MeV[17], and has an average value of 3MeV[11]. A simple visual of this concept can be seen in Figure 2 (add equation of how many events detector will see)

Figure 3: Location of detector and nuclear reactor[18]

The research done at the WATCHMAN detector will provide information to help with non-proliferation goals by advancing the ability of tracking man-made nuclear reactions. Due to the inability for neutrinos to be shielded from leaving the reactor[6] physicists, with increasing knowledge of neutrinos and better technology for detection, can use neutrino outputs to track man made nuclear reactions at large distances. This idea is currently in it's infancy however has large promise if the experimentation goes according to plan. Other detectors, such as KamLAND[8] and Double Chooz[11], have used reactor neutrinos in neutrino detector experiments previously; however, direct long-baseline experiments for non-proliferation goals with WATCHMAN's configurations have not been[8].

The proposed WATCHMAN detector in Boulby, UK will be a cylindrical tank with height and diameter of 20 metres, comprised of around 4000 10-inch diameter[1] photomultiplier tubes (PMTs). PMTs being large bulb shaped photon detectors which use the photoelectric effect. Figure 4 shows WATCHMAN's tank and detector. The tank will be filled with Gadolinium-doped water[17]. 90% of the PMTs will be facing inward viewing a a fiducial mass of around 1kT of the doped water and the remaining 10% of PMTs will face outward, to veto cosmic rays[17]. The design is similar to that of the well known water Cherenkov detector called Super-Kamiokande[19] (Super-K), located in Japan. Super-K has made many important observations about the nature of neutrinos. It was built 1km underground and contains 11200 PMTs with 20-inch diameter and is used to observe solar neutrinos[19].

The Boulby Mine is Europe's second deepest mine and has contains the Boulby Underground Laboratory[1]. The sight has 1100m of rock overhead making it a good neutrino detector host due to it providing suppression of background radiation which could mimic the neutrino signals[17]. Boulby was chosen also, due to its proximity to a nuclear reactor and its previous scientific record[1].

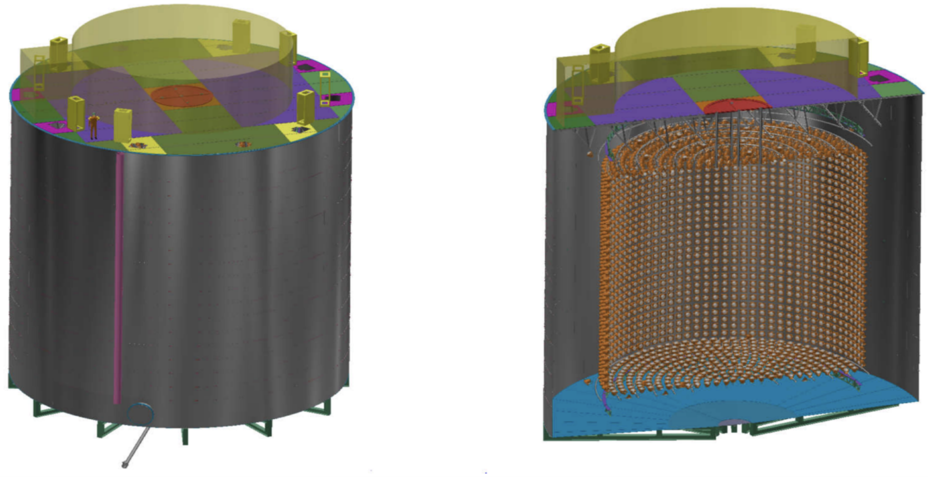

Figure 4: The WATCHMAN detector to be build at the Boulby site. The left image shows the circuitry, DAQ boxes, steel girder and the roof with a clean room. The right shows the inside of the detector with the inner PMT structure.[1]

3.1 Detector Mediums

Various methods are used to measure the output of the inverse beta decay[3]. The variations of these methods normally come down to the detector medium in which the tank is filled. There are four main techniques of neutrino detection, each with there own detector medium. These are[3]; radiochemical experiments, which use the production of radioactive isotopes; Cherenkov radiation, which use water based mediums; scintillator detectors, using the emission of gamma rays following ionisation; and tracking detectors, which use chambers to track particle trajectories. The type of medium one uses in a detector depends on the requirements of the study. Each medium has its advantages, however none can perfectly measure all aspects of a neutrino event. The desirable features of a medium include; being able to study low-energy neutrinos; good resolutions of angular trajectory, time, or energy; particle identification[3], separating the type of lepton produced from an interaction to determine the neutrino type[11]. Not all of these are achievable from one medium[11], hence, the features most important to a specific experiment must be prioritised.

Here we discuss water Cherenkov techniques, scintillation techniques, followed by a hybrid approach of the two[20]. Initially WATCHMAN was focusing on Gadolinium-doped water as its medium, however, studies into a hybrid approach of water and a liquid scintillator look promising as an alternative medium[21][22][20]. The exact use of these mediums is yet to be finalised, with a possibility of starting out with a Gd-doped water medium and changing it out for the hybrid approach later on[8][1]. The advantages and disadvantages of the mediums; water, Gadolinium doped water, and liquid scintillator can be seen in Figure 7.

3.1.1 Water and Gd-doped Water

Water is a very useful detector medium; it is abundant, cheap and has relativistic charged particles which allow for Cherenkov radiation to occur[11]. The success of the previously mentioned Super-K experiment[19] can be attributed to this water Cherenkov technique, which is a method of detection coming from Cherenkov light produced after inverse beta decay. Cherenkov light is the result of a fast moving charged particle (normally an electron or positron) travelling through a transparent, dielectric medium at speeds greater than that of the phase velocity of light in the same medium[11][23]:

$$v_{particle} > \frac{c}{n} \tag{2}$$

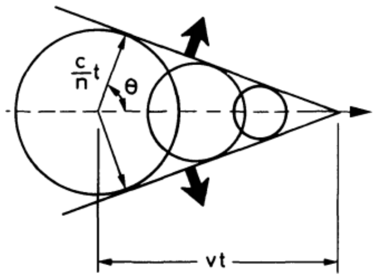

Figure 5: [23] A representation of Cherenkov radiation. A particle is travelling from left to right at speed vt through a medium of refractive index n. The cone has half angle θ which is given by $cos\theta = \frac{c}{nv}$.

The relativistic charged particle produces an electromagnetic shock wave, a coherent wavefront emitted at a well defined angle[23]. The wavefront for a particle travelling at speed vt is drawn in Figure 5 where the angle θ is dependent on the particle's speed and the frequency of the emission. The Cherenkov cone is detected as a 'ring' by the PMTs[11], with the vertex being found through the timing of light detected, the direction from the size of the cone and the energy[23] from the summed light detected. This allows for very good vertex reconstruction, much better than other detection techniques[11].

Despite the success of the Super-K experiment[19], with energy resolutions of 14.2% at 10MeV for solar and supernova experiments[24], it had a drawback due to its inability to detect thermal neutrons which helps to reduce the background noise in the detector. This being due to a flash from the positron's Cherenkov radiation followed by a neutron is a double coincidence[25] and would be very unlikely to be observed unless the inverse beta decay had occurred. Hence, only accepting detection of this signature allows for a lot more background events to be ignored. To combat this problem doped water (in WATCHMAN's case Gadolinium) is commonly used in modern Cherenkov neutrino detectors due to the increasing frequency of neutrino interaction compared to using pure water alone. Gadolinium increases detection efficiency by approximately six-fold[26], this being due to the Gadolinium nucleus having a high neutron capture cross-section, and high gamma-ray emissions from the post-excited nucleus[25]. This gamma ray emission then Compton scatters with an electron, which at high enough energies, causes it to become relativistic and emit Cherenkov radiation[26].

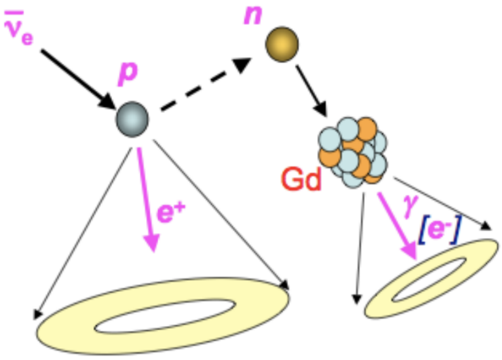

Figure 6: The inverse beta decay within Gd-doped water. Showing an anti-electron-neutrino hitting a positron causing a relativistic positron, causing Cherenkov radiation (yellow ring), and a thermal neutron. The thermal neutron is captured by a Gd-nuclei and a gamma ray emitted which undergoes Compton scattering with an electron, also causing Cherenkov radiation.[26]

The resulting gamma ray emission from a neutron capture in pure water, from the capture of a neutron by a proton, has an energy of 2.2MeV[1], this is close to the Cherenkov threshold, making it difficult to detect. Neutron capture by a Gadolinium nuclei yields a gamma cascade of 7.9MeV 80.5% of the time and 8.5MeV 19.3% of the time[1]. (Maybe add something about a gd-doped detector here)

Hence, this allows identification of anti-neutrinos via the inverse-beta decay from the signature coming from the neutron capture signal produced in coincidence with the positron signal, where the neutron capture occurs during the Compton scattering of gamma rays during the Gadolinium de-excitation. This is seen in Figure 6. For WATCHMAN Gadolinium will be loaded at a 0.1% level[1], resulting in 90% of the neutrons produced by the inverse beta decay to be captured[1].

3.1.2 Liquid Scintillator

Liquid scintillation detection techniques are very popular in neutrino physics, with the first detection of a neutrino being done in one of these types of detectors, by Reines and Cowan in 1953[27]. They can be made of a variety of materials, such as, organic liquids and plastics, inorganic crystals, and Nobel liquids. They have shown successful results and are best known through the experiments[28] Borexino[29] and KamLAND[30].

Scintillators have a high concentration of Hydrogen nuclei[28]. These nuclei act as a target for the inverse beta decay. The detection within scintillators is done through the PMTs measuring two gamma rays emitted from the annihilation of the positron, from inverse beta decay (with an electron in the scintillator)[11]. Then, after a short time, the neutron is captured, producing another gamma ray signal[28]. Isotropic light is emitted from the scintillator medium from particle ionisation[28]. The initial signal gives the anti-neutrino energy and the second signal allows for rejection of background events[28], similar to in the doped-water medium. This technique has a good time and energy resolution. This is due to scintillators tending to have much more light emission than by the Cherenkov process[28], and, unlike Cherenkov radiation, scintillation light is isotropic and has no energy threshold[28], apart from the 1.8MeV threshold for the inverse beta decay. Both KamLAND and Borexino have shown that liquid scintillators give good energy resolutions, with a 3% energy resolution at 5 MeV[28]. However, liquid scintillators do not preserve directional information.

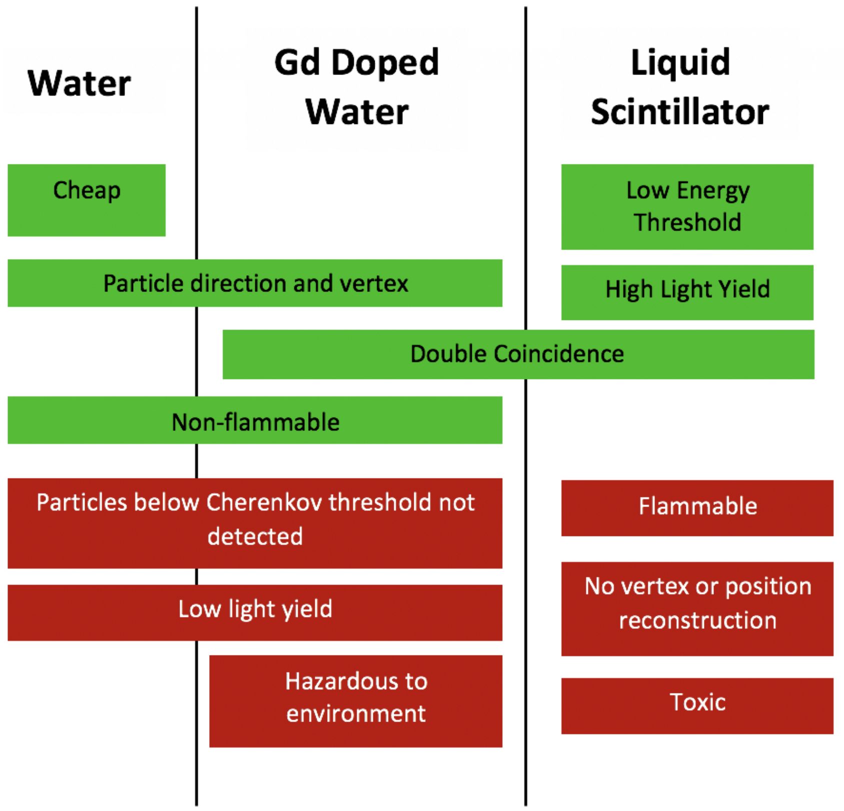

Figure 7: A table showing some of the advantages and disadvantages of pure water, Gd-doped water, and liquid scintillator as detector mediums. Water and Gd-doped water detect neutrinos through Cherenkov radiation and liquid scintillators through scintillation light. Table made in word.

3.1.3 Water based Liquid Scintillator (WbLS)

Doped-water and scintillators are two common methods of neutrino detection, however, both are with their disadvantages[21]. New mediums for neutrino detectors have been hypothesised[20]. These are hybrids of both techniques, allowing for the use of both Cherenkov light and scintillation signals[22]. These hybrids are known as Water based Liquid Scintillators, WbLS. This allows for much more accurate event classifications, as well as a clean identification of the Cherenkov cone still keeping its advantages for long-baseline neutrino physics[20]. WbLS is a simple mixture of oil (liquid scintillator) and water, typically amounts of 1-10% of liquid scintillator are introduced to the water[31]. WATCHMAN is doing experiments on WbLS concentrations of 3-5%, and in this paper a 3% WbLS medium is used. WbLS is cost effective and environmentally friendly. It includes the advantages of scintillators, having a low energy threshold and good energy resolution[20], as well as advantages of water based mediums, having low absorption as well as directional information[20]. It also has a better timing profile than both techniques using Cherenkov radiation which is fast and directional and scintillation light which is slow and isotropic[21]. Including Gadolinium doping is also possible in this medium, which could increase the resolution further. It will allow for pattern recognition far greater than in previous techniques due to the use of both signalling techniques[31]. This could increase the usefulness of machine learning (a model for pattern recognition) even greater for these detectors. WbLS will however still have to undergo purification, this is due to water losing its optical transparency over time from interactions with stainless steel in the detector[20]. This may be difficult as the method of filtration must not damage the WbLS in the process.

Due to these advantages WATCHMAN is looking into changing its plans from a Gd doped water medium to that of a Water based Liquid Scintillator. However, due to this being a fairly new area of research comparative tests need to be done in order to see if it is suitable. Other experiments are also looking into this medium[20], ANNIE at Fermilab National Laboratory are looking into making a small ton-scale detector[32], and THEIA, which is at the Long Baseline Neutrino Facility, which is aiming to build a large 25-100kt detector[31]. WATCHMAN's use of WbLS would be very helpful for future larger scale WbLS experiments.

4 Simulation of Detector and Event Reconstruction

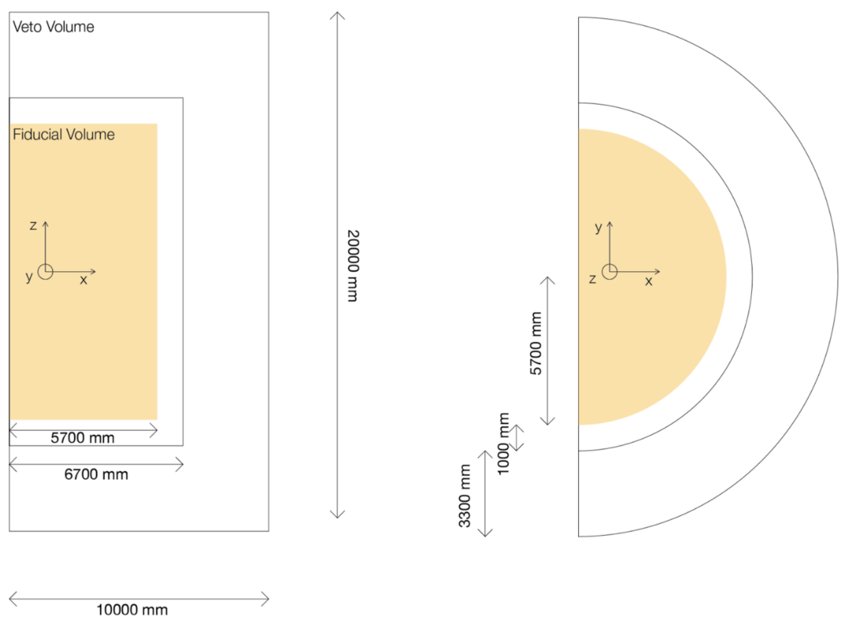

Figure 8: The geometry of WATCHMAN. Left image shows the side view of half of WATCHMAN and the right image shows the top view of half of WATCHMAN, given that the detector is cylindrical. The outer region being the veto volume and the yellow are being the fiducial volume, which is the region in which neutrino interactions are reconstructed. Made in vector works.

In optimising the characteristics of the detector and determining the effects of using different detector mediums very accurate simulations must be made. This is present before the start of any new detector project. This is due to the the detectors needing to be so sensitive and being very expensive to build. Simulations are used to optimise detector design[33]. They are expected to model gamma ray emissions, properties of the detector including geometry, particle transportation within the detector, background events, as well as the optical properties of all materials within the detector, and the PMTs[33]. In this project a particle physics simulator package called RAT-PAC[10] is being used. This is where the simulations of both the detector and the events within the detector occur. All data coming out of RAT-PAC are stored in ROOT files, as well as this all histogram plots and Gaussian fits are done within ROOT. The outputs from RAT-PAC will be the same, or similar, to the true detector. The events from the data from RAT-PAC are via a package called FRED[34]. All the simulation software and packages used for the WATCHMAN collaboration can be found on the AIT-WATCHMAN git-hub page[34].

The data from RAT-PAC/FRED is then used to train a machine learning framework (sklearn)[2] in python. This is done so to have better predictions of what is occurring in the detector by using known events with detector outputs. In this project RAT-PAC, ROOT[35], and FRED are used as they are for other areas of WATCHMAN. The machine learning part of the project will be independent study from the other members of WATCHMAN to investigate a different method of energy reconstruction.

4.1 RAT-PAC

RAT-PAC[10] (Reactor Analysis Tool Plus Additional Codes) is an analysis package originally designed for the Braidwood Collaboration and is now used in many different particle physics experiments. RAT-PAC has been modified for the Boulby detector[10][**git**], combining simulation and analysis into a single framework to allow for the same detector geometry and physical parameters to be used in a detailed simulation[10]. It takes into account the surrounding rock and walls as well as PMT type and structure[10]. It also models the triggering and data-acquisition of events, outputting data in a similar format that which WATCHMAN will measure.

RAT-PAC uses GEANT-4[36] (GEometry ANd Tracking), GLG4sim[37], ROOT[35], and C++ in performing complex Monte-Carlo simulations of the detector and the events within it[10]. SNOMAN, within the SNO Collaboration[38], inspired much of RAT[10], and the Gd capture simulation is taken from the Double-CHOOZ Collaboration[39]. RAT-PAC allows for an event to be simulated as well as all the processes that would occur in the detector after such event. After these events occur they are reconstructed via the timing and positions of photon detection by the PMTs. A virtual DAQ system is also contained within RAT, determining whether an event would cause a trigger.

The simulations which take place within RAT-PAC are controlled by macros which can set various detector geometries such as the size of the tank, the percentage coverage of PMTs, and the veto thickness of the detector. The geometry of the detector which is used in RAT-PAC can be seen in Figure 8 where the veto thickness is the outermost layer. The medium of the detector can be set within the macro as well as the type of events one wishes to simulate. Then to generate events within the detector, generators are used, they allow the user to specify the location, energy, and type of event.[10]

4.1.1 GEANT4

GEANT4 is a simulation toolkit which maps the passage of particles[36]. It was designed by an international team made up of institutes and universities. It is a large-scale object-orientated system which is adaptable, allowing it to be used for many experiments[36]. It is used in a multitude of particle and nuclear physics experiments

RAT doesn't use GEANT4 directly, instead using GLG4sim[37] (Generic Liquid-scintillator Anti-Neutrino Detector Geant4) instead[10]. It does however use GEANT4's command interpreter for interactive use and to execute macro files, as well as its compilation system and makefiles[10].

4.1.2 ROOT

ROOT[35] is a data analysis framework developed at CERN and written in C++. ROOT allows for easy to use mathematical analysis, graphing, and curve fitting[35]. It is used throughout the particle physics community and allows for collaboration of data and file formatting. Root files contain data in 'trees', these trees have substructures called 'branches' and 'leaves'. The files are able to contain massive amounts of data and plot it easily. RAT-PAC uses ROOT[35] to load and save objects[10]. All output files are given in ROOT trees.

4.2 FRED

Reconstruction of events are done through a package called FRED[34]. It inputs root files generated by RAT-PAC and reconfigures them into a format in which features of the events can be analysed. It creates an 'ntuple' data structure containing relevant data from the simulation. The FRED package is a standalone BONSAI (Branch Optimization Navigating Successive Annealing Iterations) implementation which has been reconfigured for the WATCHMAN project. FRED (BONSAI) performs a maximum likelihood fit to the timing residuals from the Cherenkov cone as well as other light signals and background to identify events and their features. These features include, for both Monte Carlo as well as their reconstructions, the number of photoelectrons , the number of PMT hits, the positional reconstructions, the timing reconstruction, and others. If the positional reconstruction of an event is outside the fiducial volume it will not be stored. The fiducial volume, shown as the yellow area in Figure 8, is the volume containing the innermost volume of water, chosen here as 1m from the PMTs to minimise the effects of radioactive interference from surrounding materials within the detector[17].

4.3 Machine Learning

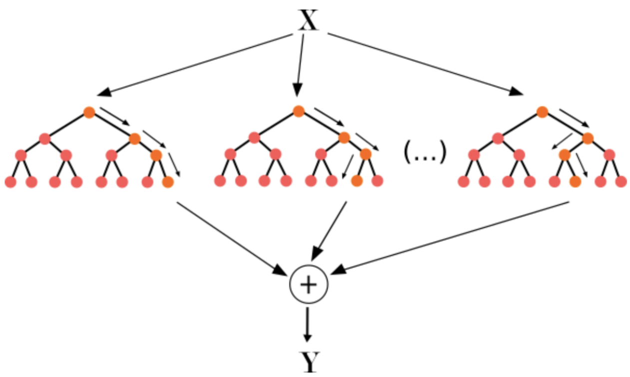

Figure 9: An example of a neural network machine learning system using multiple decision trees[40].

Throughout the development and background research performed for the WATCHMAN project traditional data analysis methods have been used. These methods are labour intensive and with large data sets become very complex[41]. This paper is set to explore the use of machine learning to better reconstruct the energy of events within the WATCHMAN detector by analysing its data outputs through a neural network[41].

Machine learning has been an increasingly popular tool for data analysis within many areas of science and technology[42]. Recently, particle physics has been using machine learning for the analysis of large data samples coming out of particle detectors[43]. It has been successfully used in experiments within the LHC (Large Hadron Collider) for event reconstruction, with important contributions being made in the discovery of the Higgs Boson[44]. An example of a neutrino experiment which uses machine learning in its analysis is NOvA at Fermi National Accelerator Laboratory[45] who use it to reconstruct and classify various neutrino events. Machine learning can be equivalent to collecting more data or being able to increase resolutions of detectors without having to build bigger, more expensive, ones. Particle physics use of machine learning is usually through neural networks, and boosted decision trees[43]. Neural networks (NN) imitate the synaptic links in the brain. Instead of synapses, NN uses a series of nodes and edges, taking inputs as real numbers and fits the data to form an output[41]. NN also use various Deep Learning (DL) hidden layers to optimise this technique[41]. An example illustration of this for one feature is seen in Figure 9

Machine learning algorithms are varied in nature and can be used in a number of different tasks[46]. They are built on a model based on a set of training data, this includes parameters which can be used for the prediction of an outcome, and the outcome itself[46]. The algorithm 'learns' from this data by recognising that some input data equates to a certain output. Machine learning models build themselves with little human intervention after the framework and data has been used[41]. The models created can be used to predict the behaviour of previously unseen data. The increasing amount of data coming out of particle physics experiments makes it unreasonable for results to be processed in a timely manner[41].

4.3.1 Gradient Boosting Regressor Algorithm

In this project the Gradient Boosting Regressor, which is a machine learning algorithm within the Scikit-Learn package[2], is used. It uses Boosted Decision Trees (BDT), converting weak learners into stronger ones[41]. Decision Trees are predictive models which go from observations about an item to conclusions about the item's target value[46].
Boosting is a general ensemble technique involving sequentially adding models which correct the performance of the previous model[46], the use of multiple decision trees in this way is known as a Random Forest. They are ideal for ensembles which use several weak learners, as they combine these weak learners into a stronger one[46]. Gradient Boosting fits the new predictor in sequence to the residual errors made by the previous predictor in the sequence[46]. From this the ensemble's prediction should gradually get better as new predictors are added. In Gradient Boosting Regressor, Regression Decision Trees are used as the base predictors[46]. The regression refers to the type of values the tree uses being continuous[46].
The Gradient Boosting Regressor class has hyperparameters[46] which, control the growth of decision trees (`max_depth`), control the ensemble training (`n_estimators`), and to scale the contribution of each tree (`learning_rate`).

5 Procedure

WATCHMAN's goal to detect Hartlepool's neutrino output requires that it has as high an energy resolution as possible. In this experiment, data was collected from various simulations of the WATCHMAN detector in RAT-PAC[10]. Events from this data was then reconstructed in the package called FRED where root files containing data trees of useful data about events within the simulation were held. Descriptions of these packages were discussed in Section 4. In this experiment positron and electron events were simulated so to better focus on the energy outputs, these being the particles which the detector will detect after a neutrino interaction[12]. The data was analysed first through conventional methods, using ROOT[35] functionality to find characteristics of the energy and positional reconstruction after the RAT-PAC output files were put through FRED. Energy was reconstructed using the mean number of photoelectrons, with the energy resolution being found by the standard deviation of the distribution of photoelectrons for a given energy. This is the current method of energy reconstruction so will be what the machine learning results will be compared to. This analysis gave the background of where to explore energy reconstruction further down the timeline of the project.

After sufficient initial analysis was completed through ROOT, the data was converted to a form that would allow it to be analysed through a machine learning algorithm. Because of the data collected the machine learning algorithm used was Gradient Boosting Regressor which is a class from scikit-learn[2]. Scikit-learn is a package for implementing machine learning within a python script. The data collected and put through the machine learning algorithm was from separate simulations of positrons and electrons within a WATCHMAN detector filled with mediums; first of Gadolinium Doped water and then of WbLS with a 3% concentration. For these different detector configurations differing energies and locations of events were implemented. The scripts made for this project can be found on git-hub [47].

5.1 Data Collection From RAT-PAC

All simulations done in this paper were done within RAT-PAC via a macro `general.mac` [47]. This macro contains the experimental parameters for the simulation. The detector experiment was set to Watchman[10] and the geometry was set to detector diameter at 20m, detector height at 20m, veto thickness as 3.3m, and the PMT coverage at 20%. This is same geometry as is seen in Figure 8. The event processor DAQ (Data AcQuisition) is used to true events into triggered events within the simulator. This matches how a real DAQ would operate[10]. In `general.mac` [47] the processor `lessimpledaq` [10] is used throughout. Finally, the generators are used to set up a series of input vectors which describe the particles to be tracked through the detector. These are split into time, position, and vertex generators[10] which decide on the rate at which the event occurs, where the event occurs, and the type/energy of the particle begins at. Finally the run function is used which causes RAT-PAC to start simulating and tells it the number of events to trigger[10]. The generators are mainly what are changed within these experiments, as well as the mediums used being described in Section 5.

The series of simulations that were made within RAT-PAC first included events within Gd-doped water. This is due to better familiarity with this medium to use as a basis of initial tests for modification of later uses. These tests were done using positrons due to their production in the inverse beta decay, however, simulations with electrons would give very similar results. Simulations using Gd-doped water were performed at discrete energy points from 1 - 10 MeV at 0.5 MeV intervals. As well as this differing PMT coverages between 0.06% - 0.5% at 4 MeV. This data was then put through FRED and analysed.

After this the `general.mac` macro was kept at 20% PMT coverage and the detector medium was changed to 3% WbLS. Data from other WATCHMAN collaborators indicated that, with the current usage of RAT-PAC, simulating electrons would be a better indication of the true events within a WbLS detector medium. Therefore, from now on electrons were simulated, however positron tests were made along the way to ensure consistency of the data. Mainly flat spectrum events were produced due to these being the most accurate data samples to train the machine learning algorithm on later. However, discrete point simulations were made also.

Simulations made in RAT-PAC throughout the project:

- Gadolinium-doped water simulations, when not specified PMT coverage is 25%
  - Positron events at the centre of the tank at discrete energy point between 2-10MeV with 0.5MeV increments. 500 runs
  - Discrete 4MeV energy positron events at the centre of the tank, varying PMT coverages between 0.06-0.5. 500 runs
  - Discrete 4MeV energy positron events at different points in tank from x,y,z = 200mm to x,y,z = 4500mm from centre of the tank. 500 runs
  - Distribution of energies between 1-10MeV, and all possible positions within the tank.
- Water-based Liquid Simulator (WbLS) simulations, when not specified PMT coverage is 20%

– 220000 electron events with distribution of energies between 1-10MeV, and all possible positions within the tank.

– Discrete 4MeV energy electron events at different points in tank from r = 500mm to r = 5000mm from centre of the tank.

5.2 Initial Results

The first simulations were done in RAT-PAC were using Gd-doped water for the medium with positron events simulated. Hence, this is the data used for the initial results. For the initial tests the trends in positional resolution and energy resolution were found for various different cases. These being; events of different MC (Monte Carlo) particle energies, events within the tank of different percentage PMT coverage, and events at differing locations in the tank. For these simulations the tank medium was Gadolinium-doped water and the events were positron particles of energies between 2-10 MeV. This was done using the trend in the number of photoelectrons measured by the detector in RAT-PAC for a given MC energy event. The initial tests were positron guns at the centre of the tank at discrete energy points. The centre of the tank will give the best resolution so will show that the detector is set up correctly if things come out as expected.

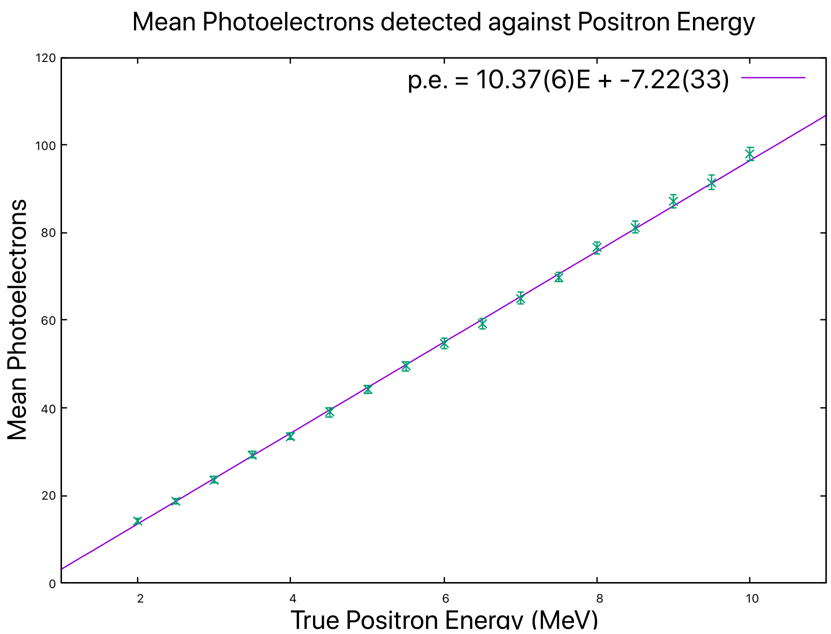

Figure 10: Trend of mean photoelectron for detected positron energies between 2 - 10 MeV within Gd-doped water at PMT coverage of 25% and events at the centre of the tank

Figure 10 shows the trend of the average number of photoelectrons detected by the PMTs versus the MC energy of the positron events. These were done at the centre of the tank and show a good correlation, implying that the simulation is calibrated sufficiently. The linear trend between photoelectrons and MC energy is what is used now

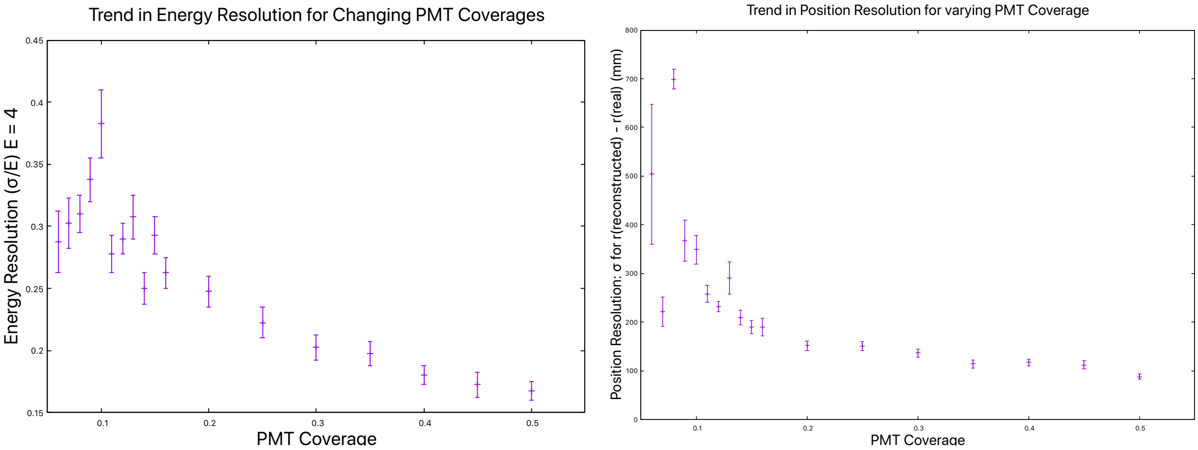

Figure 11: Tests of energy and position resolution trends for various PMT coverages of the tank.

to reconstruct energy and will be used later as one of the variables within the model. The values for the linear fit can be seen in the top right hand corner of the graph.

Figure 11 shows the energy (left) and position (right) resolutions of events within the detector at PMT coverage between 6% - 50%. These tests were done to ensure the correct PMT coverage was applied for the rest of the experiments. The simulations were done at the centre of the tank with events being positrons of energy 4 MeV.
A high percentage of PMT coverage is expensive and makes the reactor more difficult to repair. Due to this, a lower PMT coverage is preferable, however, increased PMT coverage increases the accuracy of event reconstruction. In Figure 11 it is seen that, especially for positional resolution, the gains in resolution plateau at around 20% PMT coverage. Indicating that 20% PMT coverage within the tank is an optimal value.

Figure 12 shows the trend in energy resolution based on photoelectrons for various energies of positron events within the detector. This led a good groundwork for what is expected from the rest of the study. The energy resolution is calculated by finding the standard deviation of the distribution of the number of photoelectrons for many events of the same type. A histogram of the number of photoelectrons of detected for many events at a given energy (centred at zero) was found for each case to find the appropriate standard deviation of the energy reconstruction. This was done in ROOT and a Gaussian fitted to find the appropriate values. $\frac{\sigma}{E}$ gives the fractional energy resolution, this variable is a good indication of the variability of energy reconstruction. Here it can be seen being between 14% and 32%. The idea of implementing machine learning is to have more accurate data analysis to lower these percentages.

Events within the detector have decreasing resolution as they get closer to the edge of the tank. This is due to the least amount of background radiation being at the centre of the tank. Being furthest away from the slight radiation from the detector materials. In Figure 13 this is highlighted. The resolution is worst at the edges of the detector, getting better before they plateau at around 6500mm. The mean number of photoelectrons (in blue) is shown to be higher at the edges of the tank compared to at the middle. This may make it more difficult to reconstruct energy events there due to different calibration constants, which are based on mean number of photoelectrons, will be required. Being

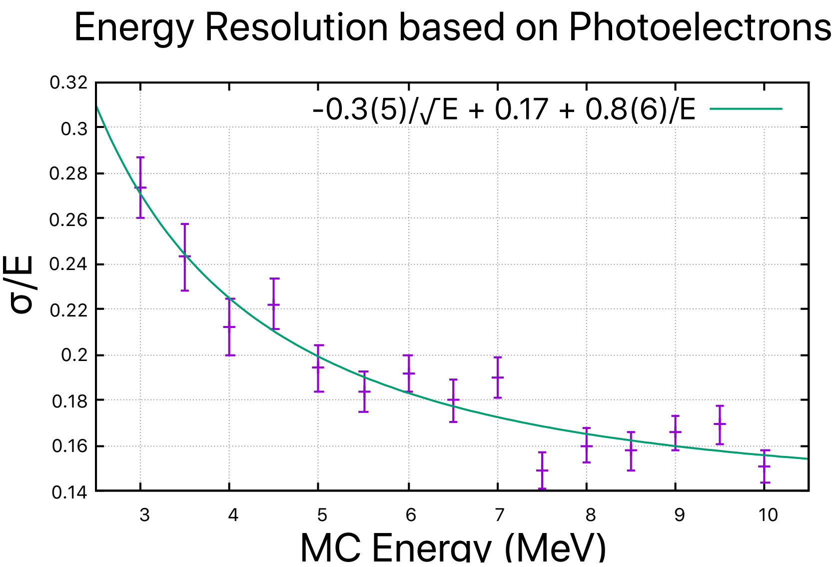

Figure 12: Trend in fractional energy resolution for events at discrete energy points between 3 - 10 MeV at the centre of the tank with Gd-doped water.

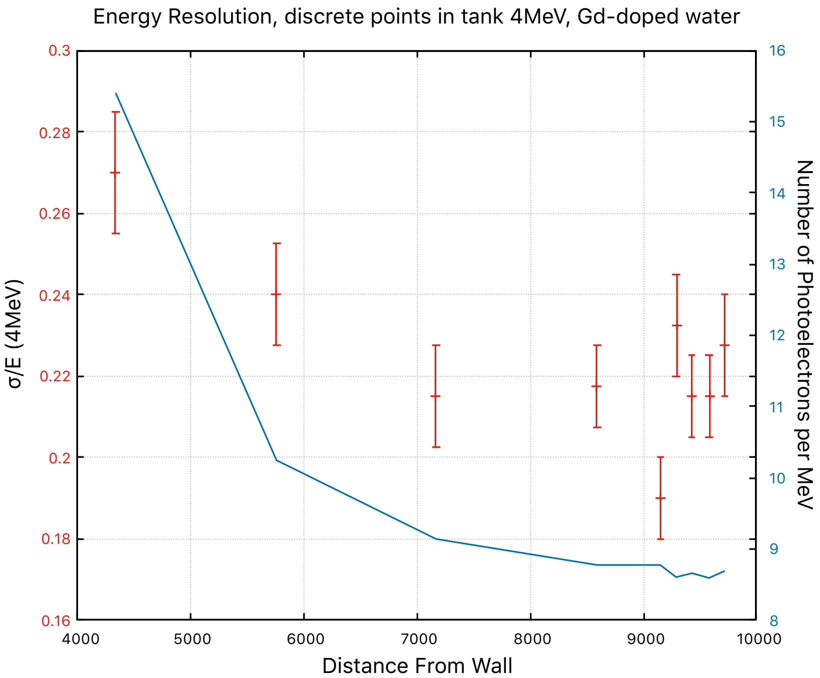

Figure 13: The energy resolution of 4MeV positron events generated at discrete points within the tank.

able to improve this variability and using a method that gives an estimated energy immediately will hopefully improved the energy resolution generally and make it quicker to calculate, with less errors. Due to this positional energy resolutions will be investigated via the machine learning method. These tests were done at 4MeV due to this being above the Cherenkov threshold and being a realistic middling energy of the expected neutrinos from the Hartlepool detector.

These findings indicate that the implementation of machine learning may increase the energy resolution found in this data. This is due to machine learning being able to use multiple variables to compute its outcome. Here, we will look at the possibility of a machine learning algorithm being able to increase energy resolution generally, as well as increasing it in the edges of the tank, to make energy resolution more uniform throughout the tank for better use of the space within the detector.

5.3 Use of Machine Learning

The data reconstructed from FRED was re-formatted and converted into csv files. The relevant data trees from the root files were extracted and only appropriate events were kept. The distance from the walls of the detector were calculated for each event and only events that were greater than 4300mm from the wall were kept. This is due to the light from events closer to the wall than this not being correctly detected. This 4300mm is made up of 3300mm from the veto volume and 1000mm as a buffer zone around the PMTs. Events further from the wall than 4300mm are in the fiducial volume, which is where events are kept. The variables from the root files that were used for input into the machine learning algorithm were; the number of photoelectrons (pe), the number of hits in 100ns (n100), the distance to the wall (reco_wall_z / reco_wall_r), and the Monte Carlo electron energy (mc_energy). The expectation is that events closer to the centre of the tank will have more accurate reconstruction, hence although the position will not be correlated with the true energy it may help the machine learning algorithm with determining the energy based on this data.

Each data file was split in two, randomly selecting half of the data which will initialise the algorithm, teaching the framework the data. The other half was used after the algorithm was trained, giving it data to predict the energy of.
70% of the data supplied initially was used to train the framework and the remainder for testing. The data was put through a Gradient Boosting Regressor[2] framework, explained in Section 4.3.1. The best performance was found to be for hyperparameters parameters of; `maximum_depth` of 10 for an individual regression of 600 `n_estimators` and a `learning_rate` of 0.01. This was found to be optimal by recording the deviance. The deviance was also used to ensure the framework wasn't being over-trained.
Then the remaining events were put through the algorithm without mc_energy data and the predictions recorded.
The data used in the model to test it initially were from a FRED reconstructed RAT-PAC simulation for a WATCHMAN detector with medium of 3% WbLS concentration. The electron events were simulated as a flat energy spectrum between 1-10MeV and flat positional spectrum within the fiducial volume.

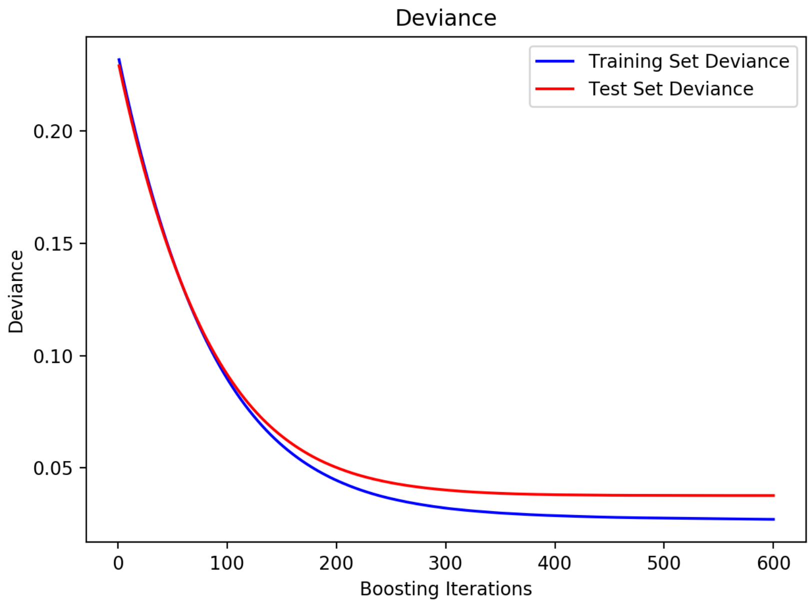

Figure 14: evolution of the least absolute deviation of the energy of simulated events during the boosting steps for the test and training samples for Scikit-Learn's Gradient Boosting Algorithm for a large number of events within 3% wbls medium of various energies between 1-10MeV throughout the tank.

Figure 14 shows the convergence of the algorithm using the least absolute deviation estimator. It is calculated by minimises the sum of the absolute values of the residuals between the true and predicted value[48]. For the model used in this project the deviation estimator was used to determine the most appropriate number of estimators and maximum depth of the model[49]. A large gap between the training deviance and test deviance can be a sign that the model is overfitting[48] and changing these variables can stop this. Over fitting is when adding more trees becomes unnecessarily complex, making the prediction accuracy worse. As well as this the mean squared error was calculated to ensure the results of the model were appropriate.

A benefit of the Gradient Boosting method is the ability to provide estimates of the importance of variables from the trained predictive model. Importance scores provide indications on how useful each feature was to the construction of the decision trees within the the model[50]. The score for each feature is calculated by the amount that it improves the performance of each decision tree. This is then averaged for all decision trees[50] in the model to give an overview across the model.
Permutation importance is found by randomly permuting the samples and finding the accuracy of the model in each case[50]. The effect on the accuracy is averaged for all the trees. This is done for each variable used in the model.

Figure 15 shows the output of the feature importance (left), and permutation feature importance (right) for

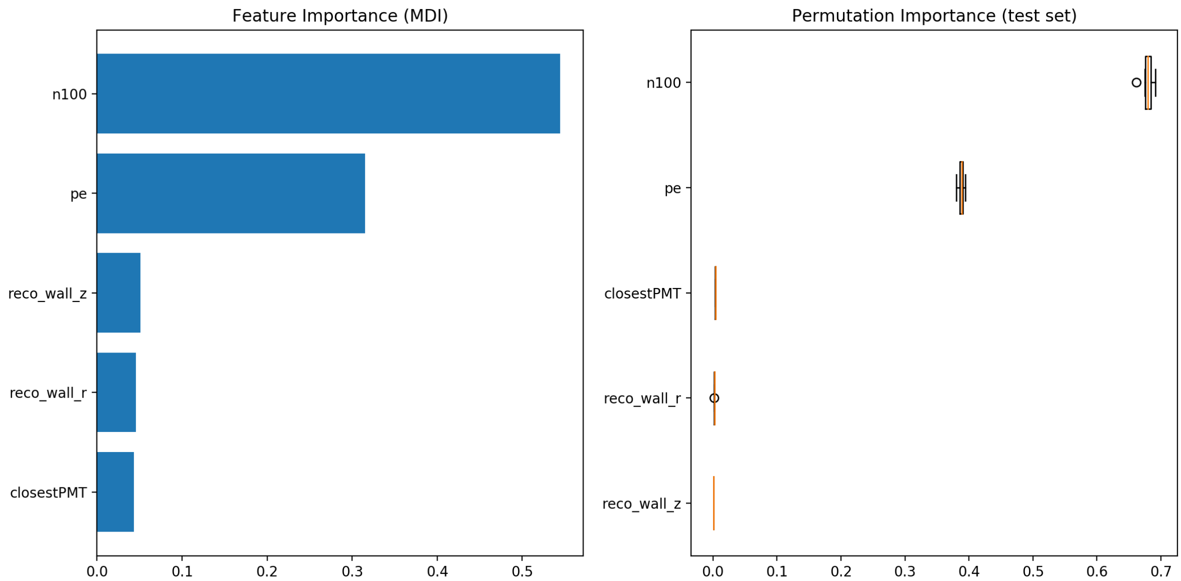

Figure 15: The Feature Importance and Permutation Feature Importance for the variables used in the model for reconstructed the energy of events.

6 Results

Simulations were executed in RAT-PAC for large numbers of runs. These runs consisted of positron events in Gd-doped water as well as electron events in WbLS. The positrons were used in Gd-doped water due to them being the particles expected for neutrino interactions in the detector. Electrons were used in WbLS due to the discovery that positrons have not been fully calibrated to the WbLS simulation yet.
The main simulation was done after the initial findings with 3% WbLS medium in the WATCHMAN detector with 0.2 PMT coverage with electron events throughout the tank's fiducial volume with energies between 1-10MeV. The energy resolutions of this run were calculated using both the photoelectron method currently being used by WATCHMAN, discussed in initial results, and the new machine learning method. These results are compared in this section to evaluate the machine learning method. All data analysis was done within ROOT and the graphs plotted were done in the plotting package gnuplot[51].

6.1 Energy Resolutions based on Energy of Events

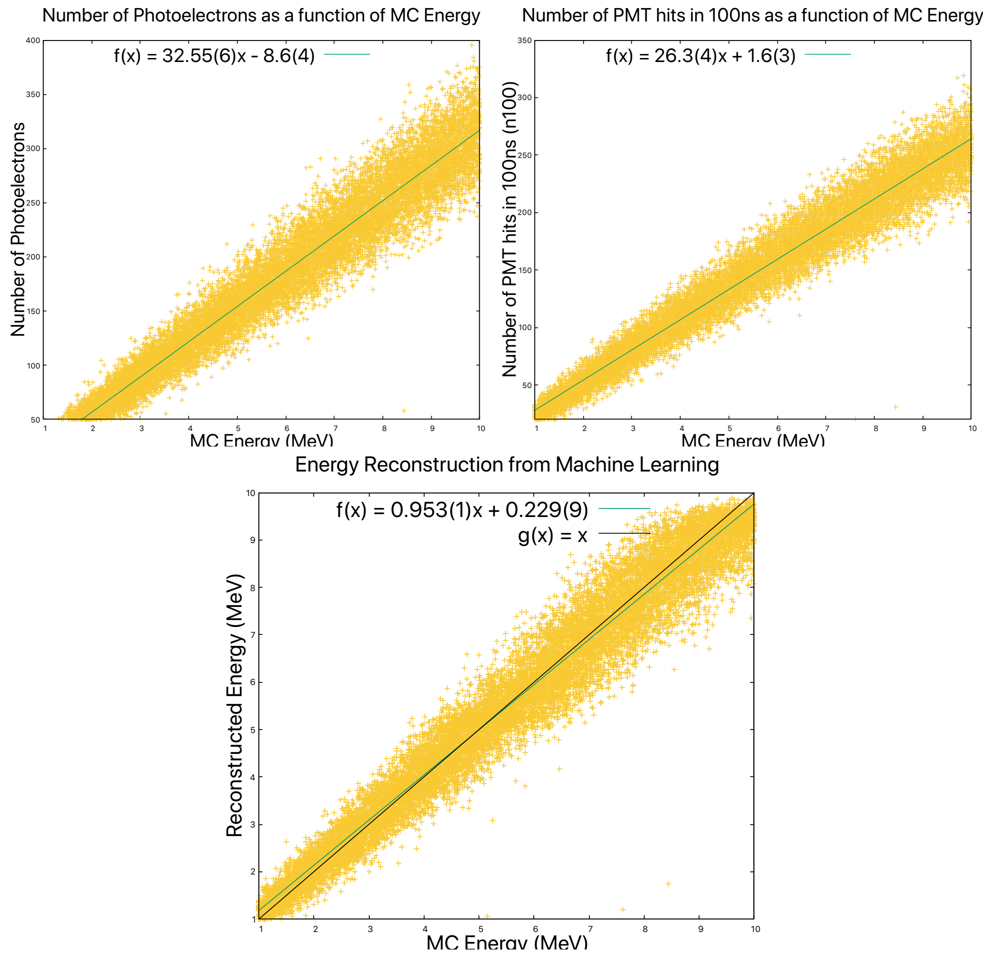

Figure 16: These graphs indicate the linear relationship of; the number of photoelectrons produced (top left); the number of PMT hits within 100ns of the event (top right); and the reconstructed energy from machine learning based on these variables (bottom) versus the monte carlo energy of electron events in the tank.

The graphs in Figure 16 show the relationships of the number of photoelectrons, the number of PMT hits, and the machine learning reconstructed energies against the Monte Carlo energy of electron events for the many event simulations described above. The top graphs (showing photoelectrons and PMT hits in 100ns respectively) show clear linear correlations, with their linear fits shown in the keys. These variables were put into the machine learning model as well as the positions of the events within the tank. The bottom graph shows the machine learning model does have a linear fit with values being close to that of the MC energy of events.

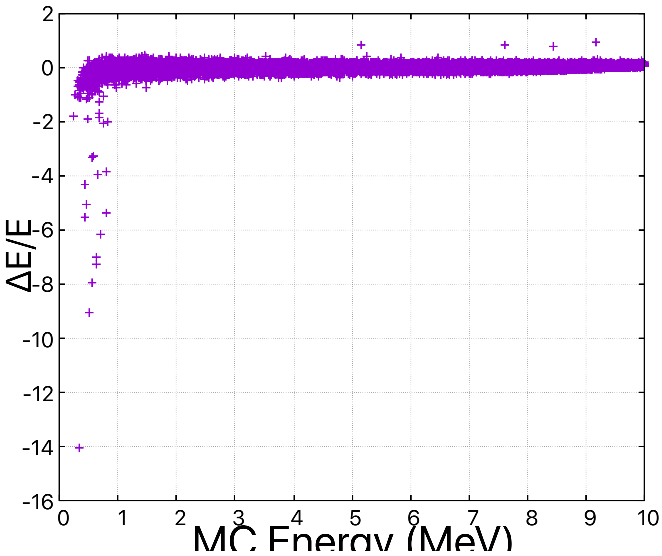

Figure 17: Fractional variation of reconstructed energy of electron events within the detector.

Figure 17 shows all of the variation of reconstructed evens for each Monte Carlo energy event.

$$\frac{\Delta E}{E} = \frac{MC_{energy} - Reconstructed_{energy}}{MC_{energy}} \tag{3}$$

This shows the fractional variation of the reconstructed energy compared to the true (MC) energy, with the perfect value being 0 for each case. Variations in the data are very large under 1MeV, this is to be expected as the detector is not calibrated as effectively for events under 1MeV. Events between 1-10 MeV are what are expected to be the energy of events in the detector. Between 1-10MeV the fractional variation is never under -1 or over +1 with the majority of events being close to zero. This is desirable and shows that the algorithm is working as expected for the data. The fractional variation is also seen decreasing as MC energy increases. A good energy resolution is defined by a low value of the standard deviation of equation 3 against MC energy.

The data from the many runs simulation of 3% WbLS were split into MC energy groups. The reconstructed data from the output of the machine learning model as well as the photoelectrons for each event were found for the events of discrete MC energy point ± 0.1 MeV. This was done for energies between 1-10MeV at intervals of 0.5 MeV. This data was then analysed in ROOT.

The fractional energy resolution was found for each of these points using the original photoelectron method, outlined in the Initial Results, Section 5.2, as well as for the reconstructed data set. The fractional energy resolution of the reconstructed energies was found via the standard deviation of equation 3. This was done in conjunction with finding the mean of each of these groups of data by plotting a histogram and fitting a Gaussian to it within ROOT. ROOT also provides the errors for these values. Plots of this data is represented in Figure 18. The top graph shows the photoelectron method in green and machine learning method in purple. These are fitted to $\frac{\sigma}{E} = \frac{a}{\sqrt{E}} + b + \frac{c}{E}$. And the bottom graph shows, in green, the mean number of photoelectrons produced per MeV of event, and in purple, the mean fractional variation of the data of each point (as represented in equation 3). The top graph shows clearly that the machine learning method is superior in energy resolution, especially for the higher energy region.

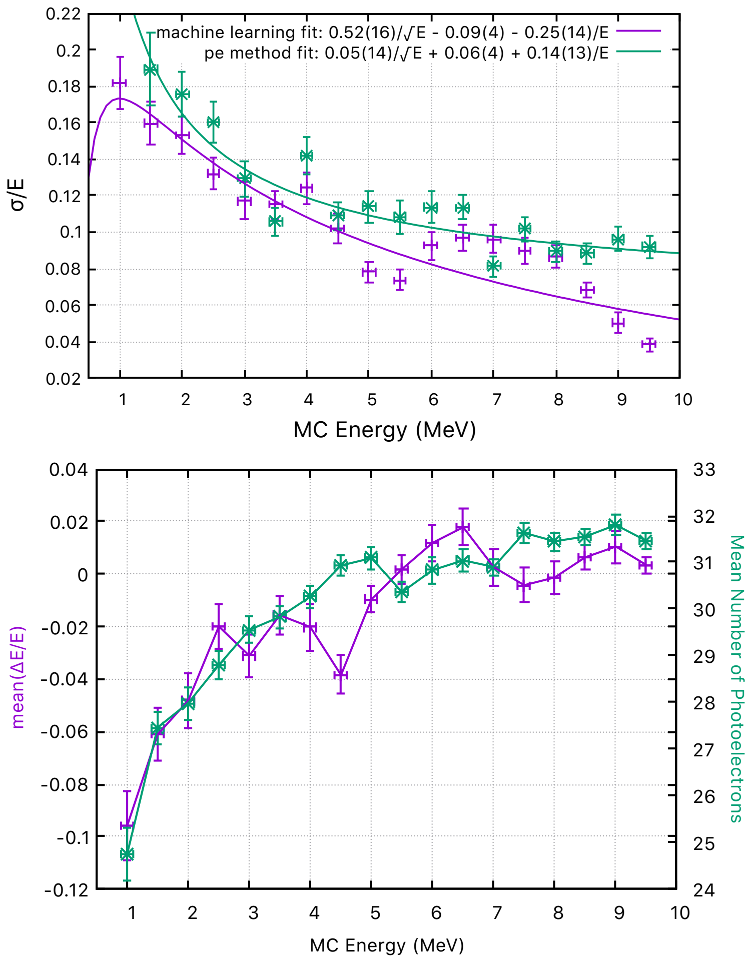

Figure 18: For WbLS medium and many runs in RAT-PAC. Top: Fractional energy resolution fitted to $f(E) = \frac{a}{\sqrt{E}} + b + \frac{c}{E}$, green showing photoelectron method and purple showing machine learning method. Bottom: Green shows the mean number of photoelectrons detected per MeV, and purple, the mean fractional variation of reconstructed energy using machine learning.

The fractional resolutions range between around 18% - 4% for the machine learning method, and between 24% - 9% for the photoelectrons method. The machine learning method may be fitted better with a linear fit with the resolutions being closest to the photoelectron method within 2.5 - 4 MeV. The gains were not as great as originally expected, however, this is a good start to the use of machine learning in WATCHMAN. There are not many literature values to compare these values with due to WbLS being a new neutrino detector medium. Boreximo[29] has some of the highest energy resolutions seen in neutrino detection with resolutions of 1% - 5% at lower energies than those seen here. Boreximo has a high light yield and a pure scintillator medium[29] which accounts for this higher resolution. Compared to Super-K, these results are much improved, with

Super-K getting to resolutions of 10% at energies of 30MeV[19]. This shows that the results of energy resolution found so far are reasonable results when compared to previous data.
The mean difference in $\frac{\sigma}{E}$ for the two methods is 0.022 with a standard deviation of 0.019. This means that there is a mean gain in energy resolution of $2.2 \pm 1.9\%$ using the machine learning method compared to the photoelectron method in this case.

The bottom graph in Figure 18 shows that the mean fractional variation from the true energy has the same trend as the mean number of photoelectrons per MeV. The fractional variation fluctuates about zero above 5 MeV; this is also where the change in the mean number of photoelectrons is between 30 and 32.

The calibration constant is found via the mean number of photoelectrons detected for each energy and hence large variations in it will make it more difficult to calculate the reconstructed energy using the photoelectrons method.

The data from the discrete energy points at the centre of the tank filled with Gd-doped water, discussed in the Initial Results section, were also put through the machine learning model. The machine learning model, in this case, was trained on data from all areas of the tank and all energies. Figure 19 shows the results from this compared to that of the photoelectrons method in the same way as was shown in Figure 18. Using the photoelectron method the the resolution ranges from just above 30% at 2.5 MeV to around 15% at 10 MeV. This resolution is worse than that found in WbLS using the same method despite the events taking place in the centre of the tank (where the reconstruction is said to be easiest). This shows that the use of WbLS is a better detector medium for WATCHMAN in terms of energy reconstruction which is what was expected. The machine learning curve (purple) has a similar comparison as it did for the WbLS with better resolutions being found generally with the most gain being seen at the lower and upper energy values. The machine learning fractional resolutions are closer together with a less obvious trend than the photoelectrons method ranging between 20% and 5%.

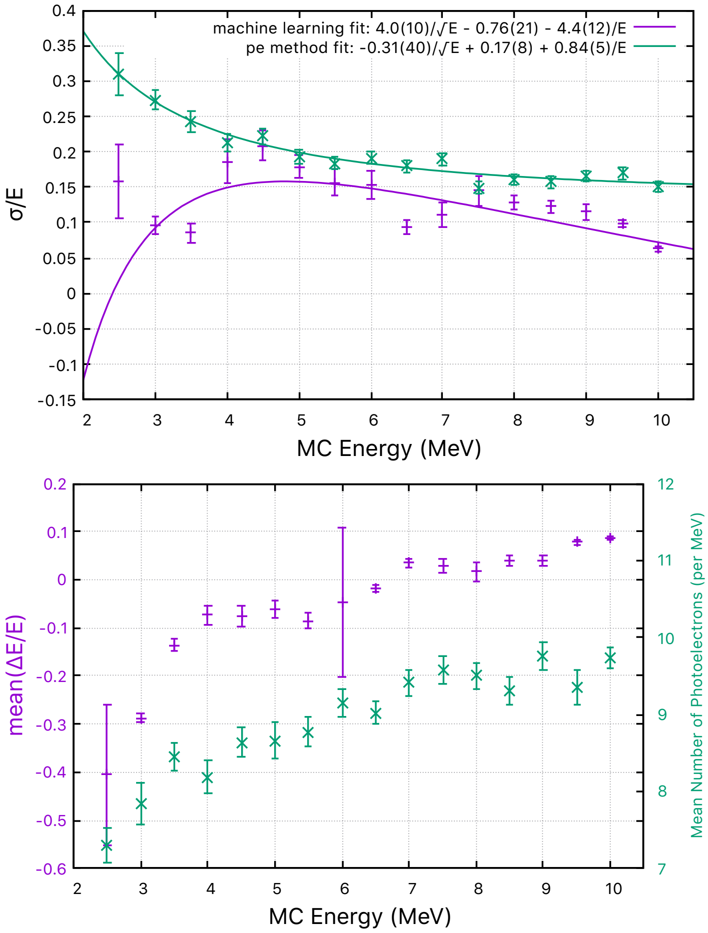

Figure 19: For Gd-doped water medium and many runs in RAT-PAC. Top: Fractional energy resolution fitted to $f(E) = \frac{a}{\sqrt{E}} + b + \frac{c}{E}$, green showing photoelectron method and purple showing machine learning method. Bottom: Green shows the mean number of photoelectrons detected per MeV, and purple, the mean fractional variation of reconstructed energy using machine learning.

The mean difference in $\frac{\sigma}{E}$ for the two methods is 0.066 with a standard deviation of 0.053. This means that there is a mean gain in energy resolution of 6.6 $\pm$ 5.3% using the machine learning method compared to the photoelectron method in this case. This indicated that there is a three fold increase in resolution using the machine learning method for Gd-doped water compared to for WbLS. This is to be expected due to Gd-doped water having a lower energy resolution generally than WbLS.

The bottom graph in Figure 19 shows again that the trend in mean fractional variation of the reconstructed energy follows the same trend as the mean number of photoelectrons per MeV. The variation is higher for Gd-doped water compared to that in WbLS with the values never being higher that 0.02 or lower than -0.1 in WbLS and are seen going as high as 0.1 and as low as -0.4 in Gd-doped water. Further evidence for WbLS being the superior medium when looking at energy resolution alone. The mean number of photoelectrons per MeV for Gd-doped water are over 3x less than for WbLS. This is to be expected, giving confirmation that WbLS allows for scintillation light resulting in higher light levels.

The machine learning algorithm performing similarly in both cases implies that it would be an acceptable method of reconstruction whether WATCHMAN decide to go with Gd-doped water or WbLS.

6.2 Energy Resolutions based on Positions in Tank

The energy resolutions at various areas within the tank were explored. This was done in both Gd-doped water and in WbLS. This was due to the finding that the energy resolution decreased as events got closer to the edge of the tank, with energy resolutions at the edge of the fiducial volume (starting 4300mm away from the walls) being considerably worse. Initially this was investigated using the many runs WbLS simulation (used in Figures 16, 17, and 18). This data was split up into regions within the tank, going from 4000mm-9000mm away from the tank walls; this is represented in Figure 20. As well as this, simulations were run at discrete points in the tank at 4 MeV for both WbLS and Gd-doped water. Simulations over the whole tank were then used in training and the model and then the model was used to predict the discrete points.

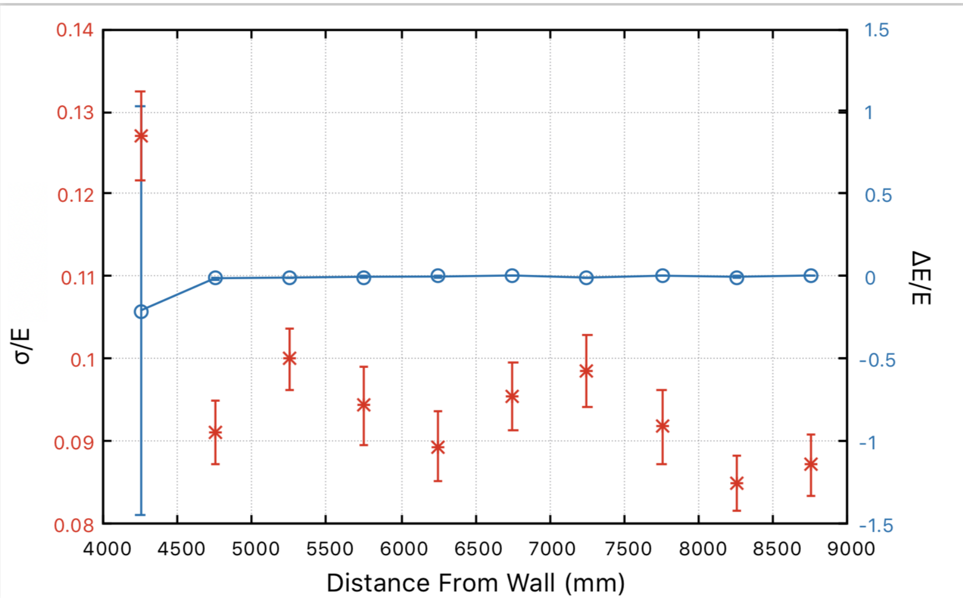

Figure 20: This graph shows the fractional energy resolution (red) and mean variational energy (blue) of the many runs RAT-PAC simulation of WbLS, based on the distance from the wall of the tank. The points being the centre of the region for which the value was found.

Figure 20 shows the energy resolutions based on areas of the tank within a WbLS medium. The fractional resolution is seen in red and remains between 8%-10% within the regions of 4500-9000mm away from the wall. The ranges at the centre of the tank were not calculated here due to not having enough data points in this area. The energy resolution is worst in the region closest to the wall, this is consistent with the initial findings and indicates that a fiducial volume starting at 4300mm from the edge of the tank is appropriate. The data point shown in this region is 4000-4500mm which is mainly out of the fiducial volume. The resolutions between 4500-9000mm vary less than was seen in initial results, possibly showing that the machine learning model is better at reconstructing energies of events further from the centre of the tank than the previously used method. Comparing this to the top graph in Figure 18 it is clear that these results are consistent. The range of resolutions within the 4500-9000mm regions are consistent with the average energy resolutions of all the discrete energy points. In Figure 20, each data point used all energies in the calculation and in Figure 18, all areas of the tank were used in the calculation of data points.

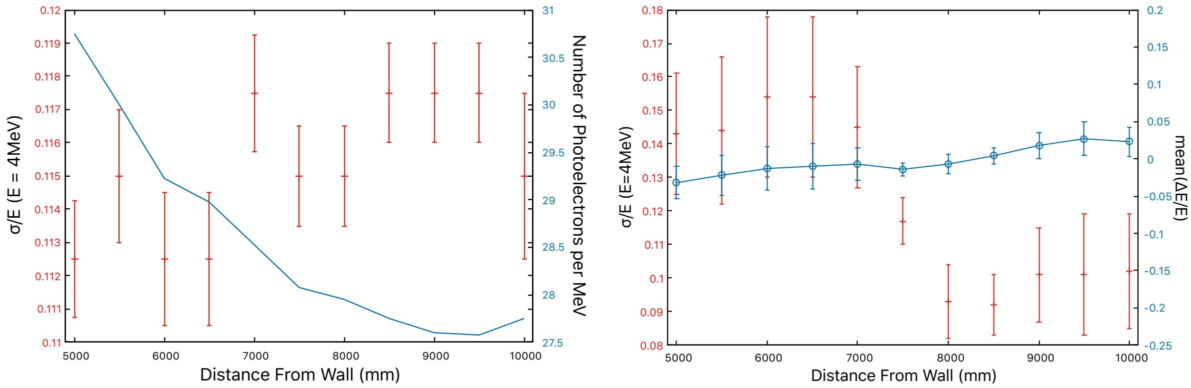

Figure 21: Graphs showing the fractional resolution and mean number of photoelectrons per MeV (left)/ fractional variations of energy (right) for 4MeV electron events at discrete points within the tank filled with a WbLS medium. The left graph indicates this using the photoelectron method and the right via the machine learning model.

As well as using the many run model to calculate energy resolutions for various radii of the tank, simulations at discrete points were also made. Figure 21 shows the data taken from 4MeV electron events at discrete points in the tank within a 3% WbLS medium. These were done within the fiducial volume of the tank ranging from 5000-10000mm from the edge of the tank. The energy resolutions for the photoelectron method have a small range with points being between 11.8% and 11.2%. These energy resolutions are better than the 14% seen for the discrete energy point resolutions found in the many runs simulations. The machine learning method sees a wider range of resolutions between 16% and 9% with a clear divide above and below 7500mm from the edge of the tank. The points higher than 7500mm are consistent with Figure 20, however, the fractional resolutions seen lower than 7500mm away from the tank are much higher in this case. This indicates a possible error in the simulations done at discrete points as the machine learning model was trained with similar data in both cases, therefore, more tests of discrete points must be made. The mean number of photoelectrons seen in Figure 18 gave a value between 30-31 photoelectrons for 4MeV electrons averaged over the tank. Here it is shown that the mean number of photoelectrons per MeV for a 4MeV electron event decreases as events get closer to the center of the tank. This is to be expected, however the mean number of photoelectrons being between 31 and 27.5 is slightly lower than was indicated in the many run simulation. The mean($\frac{\Delta E}{E}$) fluctuates around zero and is hence a more consistent value than the mean number of photoelectrons. This is consistent with Figure 20 although it shows slightly more variation. The mean fractional variation being more consistent throughout the tank than the mean number of photoelectrons is a good indicator that the machine learning method of energy resolution is superior due the changing of mean photoelectrons requiring differing calibration constants for areas within the tank.

When doing the same process as discussed for Figure 21 but with Gd-doped water, the mean fraction variation of events for each point in the tank (apart from the point between 8000-9000mm) was between -0.4 - -0.6. This indicates that there was a problem with the calibration due to all points being off what was expected by a similar value. Figure 22 indicates the non-zero peak seen in values of fractional variation of energy.

The mean number of photoelectrons per MeV is also shown to be inconsistent with the previous measurements of photoelectrons at 4MeV with Figure 19 showing around 8 photoelectrons per MeV. Figure 23 shows the number of photoelectrons per MeV being between 15.5 and 8.5, all of these values being higher than the mean of 8 photoelectrons seen previously. This may account for the strange in results shown in the machine learning data.

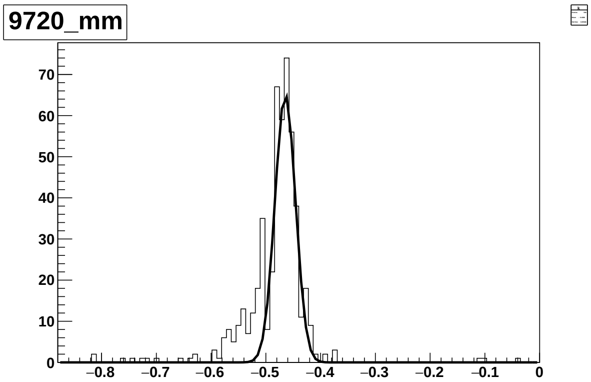

Figure 22: A graph showing the ROOT output of a fitted Gaussian to a histogram of the fractional energy variation of positron events in Gd-doped water at 9700mm away from the edge of the tank.

Despite this, the trends can still give useful insights into how well Gd-doped water does compared to WbLS, the changes in energy resolution as a function of distance from the wall of the tank, as well as the effectiveness of machine learning in energy reconstruction and whether it should be implemented into WATCHMAN.

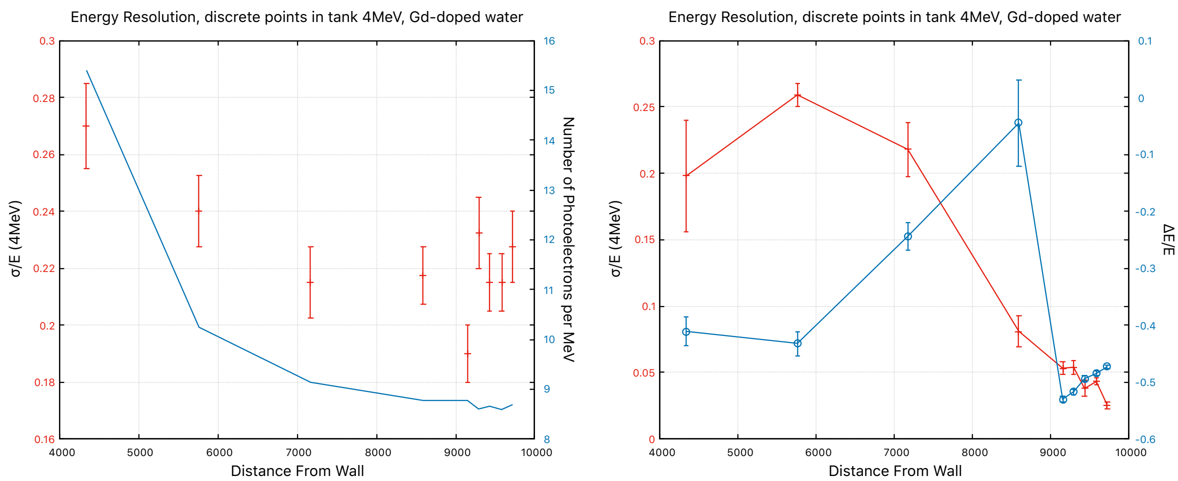

Figure 23: Graphs showing the fractional resolution and mean number of photoelectrons per MeV (left)/ fractional variations of energy (right) for 4MeV positron events at discrete points within the tank filled with a Gd-doped water medium. The left graph indicates this using the photoelectron method and the right via the machine learning model.

The machine learning methods see significant gains in energy resolution compared to the photoelectron method in Figure 23, especially for events close to the centre of the tank, going as low as 3%. This is a significantly better result than the 23% fractional resolution seen for the same point using the photoelectron method.

7 Discussion

Despite the data values in the discrete points being inconsistent, the trends show that machine learning will be a useful tool in finding energy for the events within the WATCHMAN detector. The results from the many run simulation show the most accurate results for discrete values and hence imply that more testing should be done with this technique rather than simulations at discrete points. This will also be more similar to actual events in the WATCHMAN detector when it is complete.

The results show a clear increase in energy resolution using WbLS than Gd-doped water. This indicates that from an energy reconstruction stand point WbLS will give better results than Gd-doped water. The gain in energy resolution using the machine learning method for Gd-doped water was greater than for WbLS, however, increases were seen in both showing that this method of reconstruction of energy of the events in the WATCHMAN detector could be implemented into the data analysis of the outputs. The energy resolution was also calculated at various points in the tank using both methods. These results did not show as clearly the benefit of machine learning, however, this may have been due to an error in the simulations for discrete points. This is indicated by the many runs simulation for WbLS showing very clear results. The many runs simulation that was split up into radii in Figure 20 indicates that the current fiducial volume of 4300mm from the edge of the tank is a reasonable decision.

More experiments should be done for the points within the tank for both WbLS and Gd-doped water to ensure the findings in this paper are correct. Increasing the number of events for each discrete point will make it clearer to see what is happening. Also, more simulations of events should be done generally to train and test the machine learning model. It would also be useful to use data from operating neutrino detectors, similar to WATCHMAN, to see if the model works well with real data and see how close the outputs are to the current energy predictions. Machine learning is very promising in use in reconstruction generally, hence, this method could be adapted for the reconstruction of other features of events such as position, vertex, and time.

8 Conclusion

In this paper, energy resolutions were calculated from simulated electron and positron events within a simulated version of a neutrino detector being built in Boulby, UK called WATCHMAN. The possible use of a machine learning algorithm for the energy reconstruction of events within a neutrino detector was proposed. The simulations were carried out using a software called RAT-PAC which simulates both the detector and the events within it. The current method of finding he energy resolutions of these events is by using the mean photoelectrons produced in the detector for different event energies. The analysis of energy resolution in this paper has been done for two detector mediums: water based liquid scintillator and Gadolinium-doped water. Using these mediums the energy resolution was found using the current method as well as implementing a machine learning method. The resolutions using these two methods were calculated for differing energies and positions of events. The machine learning framework used was Gradient Boosting Regressor from the Scikit-Learn learn package.

The energy resolutions are consistently better for reconstruction using the machine learning when compared to the photoelectron method using the same data. For WbLS average gains of 2.2 ± 1.9 % were found using the machine learning method when looking at resolutions of energy points, for Gd-doped water an average gain of $6.6 \pm 5.3\%$ was found.
Both methods showed that the energy resolution was worse at the edge of the tank and that a fiducial volume of 4300mm away from the edge of the tank was suitable. The difference of energy resolution at the edge of the fiducial volume was more pronounced for Gd-doped water and while using the photoelectron method.
The results in this paper indicate that the machine learning method shows good promise for energy reconstruction for WATCHMAN. There are consistent gains in energy resolution and with further training and modification it will increase the accuracy of event reconstruction as well as making the data analysis of events faster and easier.

References

[1] A. Bernstein. "Conceptual Design Overview of the Advanced Instrumentation Testbed (AIT) and the WATer CHerenkov Monitor of ANtineutrinos (WATCHMAN)". In: (Mar. 2019). DOI: `10.2172/1544490`. URL: `https://www.osti.gov/biblio/1544490`.

[2] F. Pedregosa et al. "Scikit-learn: Machine Learning in Python". In: *Journal of Machine Learning Research* 12 (2011), pp. 2825–2830.

[3] F. Von Feilitzsch, J.-C. Lanfranchi, and M. Wurm. "Neutrino detectors". English. In: *Handbook of Particle Detection and Imaging*. Springer Berlin Heidelberg, 2012, pp. 314–345. ISBN: 9783642132711.

[4] Jonathan Burns. "Remote detection of undeclared nuclear reactors using the WATCHMAN detector". In: (2018).

[5] R. D. Mckeown. "Neutrino Experiments". eng. In: *AIP Conference Proceedings*. Vol. 1265. 1. American Institute of Physics, 2010, pp. 308–315. ISBN: 978-0-7354-0814-2.

[6] Christopher Stewart, Abdalla Abou-Jaoude, and Anna Erickson. "Employing antineutrino detectors to safeguard future nuclear reactors from diversions". eng. In: *Nature communications* 10.1 (2019), pp. 3527–10. ISSN: 2041-1723.

[7] Michel Cribier and Michel Cribier. "Neutrinos and Non-proliferation in Europe". eng. In: *Earth, moon, and planets* 99.1 (2006), pp. 331–341. ISSN: 0167-9295.

[8] M. Askins et al. "The Physics and Nuclear Nonproliferation Goals of WATCHMAN: A WAter CHerenkov Monitor for ANtineutrinos". In: (2015).

[9] Hamamatsu. *Large Photocathode area Photomultiplier Tubes*. 2019 (accessed 7 March 2020). URL: https://www.hamamatsu.com/resources/pdf/etd/LARGE_AREA_PMT_TPMH1376E.pdf.

[10] *RAT (is an Analysis Tool) User's Guide*. URL: https://rat.readthedocs.io/en/latest/.

[11] P. Lipari. "Introduction to neutrino physics". In: *1st CERN-CLAF School of High-Energy Physics*. May 2001.

[12] Vernon Barger, Danny Marfatia, and Kerry Whisnant. "Neutrino Basics". eng. In: *The Physics of Neutrinos*. Princeton: Princeton University Press, 2012, pp. 11–32. ISBN: 1400845599.

[13] Alessandro De Angelis and Mário João Martins Pimenta. "The Properties of Neutrinos". eng. In: *Introduction to Particle and Astroparticle Physics*. Undergraduate Lecture Notes in Physics. Milano: Springer Milan, 2015, pp. 505–536. ISBN: 9788847026872.

[14] Pablo Fernandez. "Neutrino Physics in Present and Future Kamioka Water-Cherenkov Detectors with Neutron Tagging". PhD thesis. Feb. 2017. DOI: 10.13140/RG.2.2.19649.56169.

[15] Evgeny Akhmedov. "Relic neutrino detection through angular correlations in inverse -decay". In: *Journal of Cosmology and Astroparticle Physics* 2019.09 (Sept. 2019), pp. 031–031. DOI: 10.1088/1475-7516/2019/09/031. URL: https://doi.org/10.1088/1475-7516/2019/09/031.

[16] Muriel Fallot. "Getting to the Bottom of an Antineutrino Anomaly". eng. In: *Physics (College Park, Md.)* 10 (2017). ISSN: 1943-2879.

[17] Christopher Grant. "WATCHMAN: A Remote Reactor Monitor and Advanced Instrumentation Testbed". In: *J. Phys. Conf. Ser.* 1468.1 (2020). Ed. by Masayuki Nakahata, p. 012182. DOI: 10.1088/1742-6596/1468/1/012182.

[18] URL: https://www.google.com/maps/place/Hartlepool+Power+Station/@54.6354913,-1.3211829,11z/data=!4m5!3m4!1s0x487ef22546e4a235:0xc8916c6d5fb9ba37!8m2!3d54.6354913!4d-1.1811072.

[19] M.B Smy. "Low Energy Challenges in Super-Kamiokande-III". eng. In: *Nuclear physics. Section B, Proceedings supplement* 168 (2007), pp. 118–121. ISSN: 0920-5632.

[20] J. R Alonso et al. "Advanced Scintillator Detector Concept (ASDC): A Concept Paper on the Physics Potential of Water-Based Liquid Scintillator". eng. In: (2014).

[21] D. Beznosko et al. "Performance of Water-Based Liquid Scintillator: An Independent Analysis". English. In: *Advances in High Energy Physics* 2014 (2014). URL: https://search-proquest-com.ezproxy.is.ed.ac.uk/scholarly-journals/performance-water-based-liquid-scintillator/docview/1552843689/se-2?accountid=10673.

[22] B. J. Land et al. "MeV-scale performance of water-based and pure liquid scintillator detectors". In: *Phys. Rev. D* 103 (5 Mar. 2021), p. 052004. DOI: 10.1103/PhysRevD.103.052004. URL: https://link.aps.org/doi/10.1103/PhysRevD.103.052004.

[23] William R. Leo. *Techniques for nuclear and particle physics experiments : a how-to approach*. eng. Second revised edition.. Berlin ; London: Springer-Verlag, 1994. ISBN: 3540572805.

[24] Suzuki, Yoichiro. “The Super-Kamiokande experiment”. In: *Eur. Phys. J. C* 79.4 (2019), p. 298. DOI: 10.1140/epjc/s10052-019-6796-2. URL: https://doi.org/10.1140/epjc/s10052-019-6796-2.

[25] “Double Chooz 13 measurement via total neutron capture detection”. In: *Nature Physics* 16.5 (Apr. 2020), pp. 558–564. ISSN: 1745-2481. DOI: 10.1038/s41567-020-0831-y. URL: http://dx.doi.org/10.1038/s41567-020-0831-y.

[26] Luis Labarga. “About a Gadolinium-doped Water Cherenkov LAGUNA Detector”. eng. In: *AIP Conference Proceedings* 1304.1 (2010). ISSN: 0094-243X.

[27] F Reines and C.L Cowan Jr. “Detection of the free neutrino”. eng. In: *Physical review* 92.3 (1953), pp. 830–831. ISSN: 0031-899X.

[28] Michael Wurm et al. “The next-generation liquid-scintillator neutrino observatory LENA”. In: *Astroparticle Physics* 35.11 (2012), pp. 685–732. ISSN: 0927-6505. DOI: https://doi.org/10.1016/j.astropartphys.2012.02.011. URL: https://www.sciencedirect.com/science/article/pii/S0927650512000503.

[29] G. Alimonti et al. “The Borexino detector at the Laboratori Nazionali del Gran Sasso”. In: *Nuclear Instruments and Methods in Physics Research Section A: Accelerators, Spectrometers, Detectors and Associated Equipment* 600.3 (Mar. 2009), pp. 568–593. ISSN: 0168-9002. DOI: 10.1016/j.nima.2008.11.076. URL: http://dx.doi.org/10.1016/j.nima.2008.11.076.

[30] F. Suekane et al. “An overview of the kamland 1-kiloton liquid scintillator”. In: *KEK - RCNP International School and Miniworkshop for Scintillating Crystals and their Applications in Particle and Nuclear Physics*. Apr. 2004. arXiv: physics/0404071.

[31] Vincent Fischer. “Theia: A multi-purpose water-based liquid scintillator detector”. eng. In: (2018).

[32] A. R. Back et al. *Accelerator Neutrino Neutron Interaction Experiment (ANNIE): Preliminary Results and Physics Phase Proposal*. 2017. arXiv: 1707.08222.

[33] Maury Goodman Thierry Lasserre. “Double Chooz, A Search for the Neutrino Mixing Angle theta-13”. eng. In: (2006).

[34] Tomi Akindele, Marc Bergevin, and Morgan Askins. *AIT-WATCHMAN*. URL: https://github.com/AIT-WATCHMAN.

[35] Rene Brun et al. *root-project/root: v6.18/02*. Version v6-18-02. Aug. 2019. DOI: 10.5281/zenodo.3895860. URL: https://doi.org/10.5281/zenodo.3895860.

[36] S. Agostinelli et al. “Geant4—a simulation toolkit”. In: *Nuclear Instruments and Methods in Physics Research Section A: Accelerators, Spectrometers, Detectors and Associated Equipment* 506.3 (2003), pp. 250–303. ISSN: 0168-9002. DOI: https://doi.org/10.1016/S0168-9002(03)01368-8. URL: https://www.sciencedirect.com/science/article/pii/S0168900203013688.

[37] Glenn Horton-Smith. *GLG4sim: Main Page*. 2021. URL: https://www.phys.ksu.edu/personal/gahs/GLG4sim/docs/html_latest/index.html.

[38] Philip G Jones. *Background rejection for the neutrinoless double beta decay experiment SNO*. eng. 2011.

[39] Dario Motta and Anatael Cabrera. "The Double Chooz simulation strategy". eng. In: *Nuclear physics. Section B, Proceedings supplement* 221 (2011), pp. 378–378. ISSN: 0920-5632.

[40] Ramraj Chandradevan. *Random Forest Learning-Essential Understanding*. Aug. 2017. URL: `https://towardsdatascience.com/random-forest-learning-essential-understanding-1ca856a963cb`.

[41] Dimitri Bourilkov. "Machine and Deep Learning Applications in Particle Physics". In: *Int. J. Mod. Phys. A* 34.35 (2020), p. 1930019. DOI: `10.1142/S0217751X19300199`. arXiv: `1912.08245 [physics.data-an]`.

[42] Greig Cowan et al. *Machine Learning-based Energy Reconstruction for Water-Cherenkov detectors*. 2017. arXiv: `1704.08898 [physics.ins-det]`.

[43] Alexander Radovic et al. "Machine learning at the energy and intensity frontiers of particle physics". eng. In: *Nature (London)* 560.7716 (2018), pp. 41–48. ISSN: 0028-0836.

[44] CMS Collaboration. "Observation of a new particle in the search for the Standard Model Higgs boson with the ATLAS detector at the LHC". In: *Physics Letters B* 716.1 (2012), pp. 1–29. ISSN: 0370-2693. DOI: `https://doi.org/10.1016/j.physletb.2012.08.020`. URL: `https://www.sciencedirect.com/science/article/pii/S037026931200857X`.

[45] Pierre Baldi et al. "Improved energy reconstruction in NOvA with regression convolutional neural networks". eng. In: *Physical review. D* 99.1 (2019). ISSN: 2470-0010.

[46] Aurélien Géron. *Hands-on machine learning with Scikit-Learn and TensorFlow : concepts, tools, and techniques to build intelligent systems*. eng. Sebastopol, CA: O'Reilly Media, Incorporated, 2017. ISBN: 9781491962268.

[47] Dorman-Gajic Larisa. $ml_watchman$. 2021. URL: `https://github.com/LariDG/ml_watchman`.

[48] L. Wang, M. D. Gordon, and J. Zhu. "Regularized Least Absolute Deviations Regression and an Efficient Algorithm for Parameter Tuning". In: *Sixth International Conference on Data Mining (ICDM'06)*. 2006, pp. 690–700. DOI: `10.1109/ICDM.2006.134`.

[49] V. Kishore Ayyadevara. *Pro Machine Learning Algorithms: A Hands-On Approach to Implementing Algorithms in Python and R*. eng. 1st ed. Berkeley, CA: Apress L. P, 2018. Chap. Gradient Boosting Machine. ISBN: 1484235630.

[50] Leo Breiman. "Random Forests". eng. In: *Machine learning* 45.1 (2001), pp. 5–32. ISSN: 0885-6125.

[51] Thomas Williams, Colin Kelley, and many others. *Gnuplot 4.6: an interactive plotting program*. `http://gnuplot.sourceforge.net/`. Apr. 2013.